3.4 THz quantum cascade laser operating above liquid nitrogen temperature

B.S. Williams, S. Kumar, H. Callebaut, Q. Hu and J.L. Reno

Terahertz lasing in a quantum cascade structure in pulsed mode up to a temperature of 87K at a wavelength of $\lambda = 88$ μm (3.4 THz) has been obtained. At 5K, a peak power of approximately 3.4 mW is observed, with still ~1 mW at 78K.

Introduction: The far-infrared, or terahertz, frequency regime (1–10 THz, $\lambda = 30$–300 μm) is the subject of increasing interest for a wide variety of applications including spectroscopy and imaging. Technological development has been impeded by the lack of compact, coherent sources of radiation in this spectral region. The recent extension of quantum cascade laser (QCL) operation from the mid-infrared into the terahertz is a major step towards addressing this issue [1–3]. While both pulsed and continuous-wave operation have been achieved [4, 5], these first generation devices required operation below liquid nitrogen temperature (77K), which is inconvenient for nearly all applications. In this Letter we report lasing in pulsed mode up to 87K at 3.4 THz, equivalent to a wavelength of $\lambda = 88$ μm. Measurements can now be easily performed using a liquid nitrogen cooled source and a room temperature pyroelectric detector.

Design and fabrication: The gain region, described in detail in [3], consists of 175 cascaded four-well modules. Direct longitudinal-optical-phonon scattering coupled with resonant tunnelling is used to selectively depopulate the lower radiative state. Since this fast scattering mechanism is relatively insensitive to temperature and the electron distribution, this scheme provides a robust population inversion at elevated temperatures. This structure was grown in the $GaAs/Al_{0.15}Ga_{0.85}As$ material system on a semi-insulating GaAs wafer using molecular beam epitaxy. Optical waveguiding is provided by interface plasmon confinement between the upper metallic contact and the heavily doped contact layer ($N_D = 3 \times 10^{18}$ cm^{-3}, 0.8 μm thick) grown between the active region and the substrate [3, 6]. Non-alloyed ohmic contacts composed of Ti/Au were deposited on the low-temperature grown n++ GaAs top contact, and wet etching was used to pattern 200 μm wide ridges. Ni/Ge/Au alloyed contacts were then made to the exposed contact layer adjacent to the ridge, and the back of the 600 μm-thick substrate was coated with Ti/Au to enable soldering. The ridge was cleaved to provide a 2.56 mm-long Fabry-Perot waveguide, and the back facet was coated with evaporated Al_2O_3/Ti/Au (approximately 200/15/150 nm thickness) to provide a high reflectivity mirror. After indium soldering the devices onto a copper mount, the device was wire bonded in series with a 40 Ω chip resistor for the purposes of impedance matching. The device was then mounted on a cold finger in a liquid helium cryostat for testing.

Results: This device was tested using 200 ns-long pulses repeated at 1 kHz (corresponding to a 0.02% duty cycle) as the temperature was increased from 5 up to 87K. Longer pulses have repeatedly damaged the chip resistor. The intensity was measured using a Ge:Ga photodetector, with the input beam attenuated to prevent saturation. The absolute power was calibrated using a pyroelectric detector with the beam collected onto the 2 mm diameter detector element using a cone optic. However, the collection efficiency is significantly less than unity, so the reported uncorrected power levels understate the actual emitted power levels. Light intensity against current is shown in Fig. 1, along with the bias against current relation from a different, but typical, device. At 5K, the threshold current density was $J_{th} = 806$ A/cm^2, with a maximum of 3.4 mW peak power. At a heatsink temperature of 78K, J_{th} had increased to 904 A/cm^2, and the maximum power was approximately 1 mW. The inset of Fig. 1 shows the dependence of the threshold current density against temperature. It is common to fit the higher temperature behaviour according to the phenomenological expression $J_{th} \sim \exp(T/T_0)$. Although our device does not reach high enough temperature for a good fit, a value of $T_0 = 120$K is obtained if the highest temperature points are used.

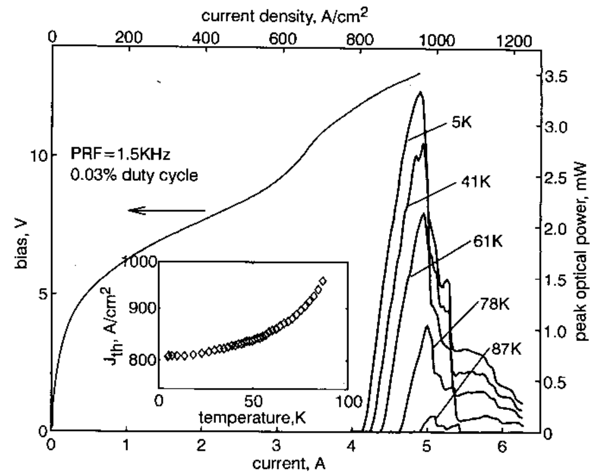

Fig. 1 *Collected optical power and applied bias against current measured with 200 ns pulses repeated at 1 kHz*

Note that bias against current curve is from a different device with smaller area, and only current density is directly comparable

Inset: Semi-log plot of threshold current density against temperature

Emission spectra were taken using 200 ns pulses repeated at 10 kHz using the Ge:Ga photodetector at the output of a Fourier transform infrared spectrometer operating with 0.125 cm^{-1} resolution. A typical emission spectrum taken at 78K is shown in Fig. 2, with the inset showing spectra taken over a range of current biases at the same temperature. The emission is largely singlemode for lower injection currents in the range where the slope of power–current relation is positive ($I \leq 4.8$ A). Beyond this range, the emission power decreases with an increasing current, as a result of the injector becoming misaligned with the upper state. Consequently, the emission spectra become increasingly multimode and shift to higher frequencies at higher currents. This blue shift of the gain is due to the Stark shift of the intersubband transition. The measured mode spacing is approximately 0.51 cm^{-1} at 5K, which corresponds to an effective mode index of $n_{eff} = 3.8 \pm 0.1$. The individual modes are continuously red shifted by roughly 0.16 cm^{-1} (4.8 GHz) as the temperature is increased from 5 to 78K.

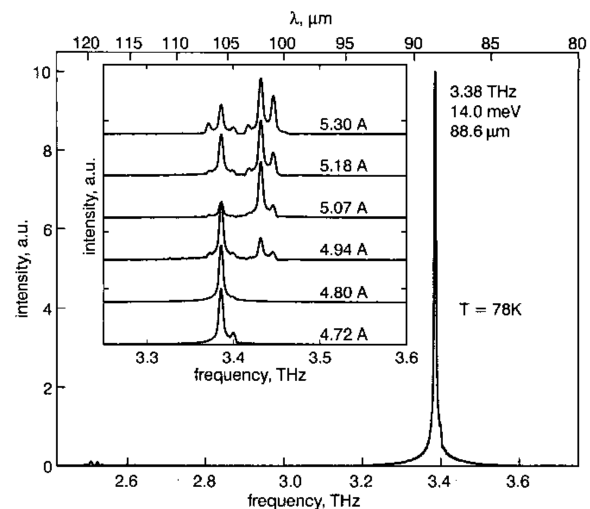

Fig. 2 *Spectrum collected from 200 μm-wide and 2.56 mm-long Fabry-Perot ridge, biased with 200 ns pulses repeated at 10 kHz with bias current of 4.80 A and collected with laser cooled by liquid nitrogen at heatsink temperature of 78K*

Inset: Spectra taken for several drive currents

The improvement in temperature performance compared to the device in [3] is due to both the increase in cavity length and width. Increasing the cavity length from 1.18 to 2.56 mm reduced the mirror

losses from $\alpha_m = 4.9\ \text{cm}^{-1}$ to $\alpha_m = 2.2\ \text{cm}^{-1}$. The threshold condition for lasing is $\Gamma g = \alpha_m + \alpha_w$, where Γ is the modal confinement factor and α_w is the waveguide loss. Using calculated values of $\Gamma = 0.29$ and $\alpha_w = 7.1\ \text{cm}^{-1}$ [3], this increase in cavity length therefore reduces the threshold material gain g from $41\ \text{cm}^{-1}$ to $32\ \text{cm}^{-1}$. The wider ridge also improves the device performance, primarily by providing a more uniform current distribution. The wet etch process used to define the mesa produces sloped sidewalls, and hence different modules in the active region are effectively biased at different points, which can reduce the peak available gain. This effect is made worse by the fact that below the bias point of $\sim$10 V (650 A/cm^2) (see Fig. 1) current is parasitically injected into the lower radiative state. As a result, beyond this point, the gain per module is a strong function of current, which results in an increased sensitivity of the total gain to current non-uniformity. The wider ridge may also slightly reduce the waveguide loss by reducing the lateral mode overlap with the alloyed ohmic contacts (separated from the ridge by 50 μm). These improvements were sufficient to enable the operation of terahertz lasers above liquid nitrogen temperature.

Acknowledgments: This work is supported by AFOSR, NASA, and NSF. Sandia is a multiprogram laboratory operated by Sandia Corporation, a Lockheed Martin Company, for the US Department of Energy under Contract No. DE-AC04-94AL85000.

© IEE 2003
8 April 2003

Electronics Letters Online No: 20030587
DOI: 10.1049/el:20030587

B.S. Williams, S. Kumar, H. Callebaut and Q. Hu (*Department of Electrical Engineering and Computer Science and Research Laboratory of Electronics, Massachusetts Institute of Technology, Cambridge, MA 02139, USA*)

E-mail: bwilliam@mit.edu

J.L. Reno (*Department 1123, Sandia National Laboratories, MS 0601, Albuquerque, NM 87185-0601, USA*)

References

1 KOHLER, R., TREDICUCCI, A., BELTRAM, F., BEERE, H., LINFIELD, E., DAVIES, G., RITCHIE, D., IOTTI, R.C., and ROSSI, F.: 'Terahertz semiconductor-heterostructure laser', *Nature*, 2002, **417**, pp. 156–159

2 ROCHAT, M., AJILI, L., WILLENBERG, H., FAIST, J., BEERE, H., DAVIES, G., LINFIELD, E., and RITCHIE, D.: 'Low-threshold terahertz quantum-cascade lasers', *Appl. Phys. Lett.*, 2002, **81**, pp. 1381–1383

3 WILLIAMS, B.S., CALLEBAUT, H., SUSHIL, K., HU, Q., and RENO, J.L.: '3.4-THz quantum cascade laser based on longitudinal-optical-phonon scattering for depopulation', *Appl. Phys. Lett.*, 2003, **82**, pp. 1015–1017

4 AJILI, L., SCALARI, G., HOFSTETTER, D., BECK, M., FAIST, J., BEERE, H., DAVIES, G., LINFIELD, E., and RITCHIE, D.: 'Continuous-wave operation of far-infrared quantum cascade lasers', *Electron. Lett.*, 2002, **38**, pp. 1675–1676

5 KOHLER, R., TREDICUCCI, A., BELTRAM, F., BEERE, H.E., LINFIELD, E.H., DAVIES, A.G., RITCHIE, D.A.S., DHILLON, S.S., and SIRTORI, C.: 'High-performance continuous-wave operation of superlattice terahertz quantum-cascade lasers', *Appl. Phys. Lett.*, 2003, **82**, pp. 1518–1520

6 ULRICH, J., ZOBL, R., FINGER, N., UNTERRAINER, K., STRASSER, G., and GORNIK, E.: 'Terahertz-electroluminescence in a quantum cascade structure', *Physica B*, 1999, **272**, pp. 216–218

Mid-infrared ring laser

A. Krier, V.V. Sherstnev, D. Wright, A.M. Monakhov and G. Hill

The first mid-infrared ring laser diode based on InAs and operating in the mid-infrared spectral region near 3 μm and with a maximum operating temperature of 125 K is reported. The source is based on a symmetrical double heterostructure with large band offsets.

Introduction: Semiconductor ring resonator lasers offer a range of advantages over other geometries that employ cleaved facets or gratings for optical feedback. These include ease of integration, a lack of spatial hole burning due to travelling-wave operation and narrow linewidth singlemode operation with high sidemode rejection. Until now ring lasers have been made predominantly at wavelengths < 2 μm and in GaAs/AlGaAs, using curved waveguides, as well as in InP/InGaAsP using large diameter rings or microdisks [1–6]. We have recently obtained superluminescence from LEDs with a ring contact configuration operating at 3.3 and 4.6 μm with characteristic spectral line narrowing [7–9]. In this case the superluminescence in the edge emission originates from in-plane propagation of the light around the inside perimeter of the mesa due to a 'whispering gallery' mode which is facilitated by total internal reflection. In this Letter we report the first mid-infrared diode ring laser based on this concept, operating in InAs near 3 μm.

Experimental procedures: The laser diodes were fabricated from double heterostructures (DHs) grown by liquid phase epitaxy (LPE) using a conventional horizontal, multi-well graphite sliding boat. Epitaxy was carried out with the boat inside a high purity quartz reactor tube using ultra-pure flowing hydrogen gas from a Pd-diffusion unit. The resulting epitaxial DH structure comprised an unintentionally doped n-InAs active layer enclosed between P- and N-InAsSbP confinement layers. The P content in the confinement layers was 0.40 ($Eg = 630$ meV, $T = 77$K) to provide higher bandgap energy and large interface band offsets for good carrier confinement. The InAs active region was 0.7 μm thick ($Eg = 414$ meV, $T = 77$K), and the InAsSbP layers were iso-periodic with InAs and each 3 μm in thickness. By using Yb rare earth gettering the residual carrier concentration in the active layer was reduced to $< 5 \times 10^{15}\ \text{cm}^{-3}$ at 300K, whereas the cladding layers were doped with Sn up to a concentration of $5 \times 10^{18}\ \text{cm}^{-3}$ and with Zn up to $1 \times 10^{18}\ \text{cm}^{-3}$ for N- and P-sides, respectively. The epitaxial structures were grown onto (100) oriented InAs substrates obtained from Wafer Technology Ltd.

Ring resonator diodes were fabricated from the epitaxial wafers using conventional photolithography and reactive ion etching with CH_4:H_2 followed by passivation with Si_3N_4 to produce mesas 420 μm in diameter. A 300 μm diameter ohmic ring contact pad (30 μm width) was defined on the n-$InAs_{0.42}Sb_{0.18}P_{0.40}$ while the corresponding back contact was deposited over the entire rear surface of the chip.

The electroluminescence emission spectra from the laser diodes and light-current characteristics were typically measured at 77K using 2 μs current pulses of up to 4 A and a frequency of 30 kHz. The electroluminescence was collected using CaF_2 lenses, focused into a 1 m Monospek 1000 monochromator and detected using a cooled (77K) InSb photodiode detector and Stanford Research (SR850) digital phase-sensitive detector. A computer was used to control the monochromator and record the final signal using *Labview* operating software.

Results and discussion: Coherent emission was obtained at 3.017 μm at 81.4K as shown in the electroluminescence spectrum of Fig. 1. Similar optical resonant mode behaviour has been observed previously in microdisk lasers [5, 10] and LEDs operating at much shorter wavelengths [6, 11]. It has been shown that such a microdisk cavity may support two different resonant mode types; radial and whispering gallery modes (WG) [12]. Radial modes are dominated by photon wave motion along the radial direction of the disk, the equivalent cavity being formed between the edge and the centre of the disk. These radial oscillations are unlikely, in our case, due to the ring contact and local current crowding which prevents such propagation.

Conversely, the WG mode may be thought of as in-plane propagation around the inside perimeter of the disk, or mesa in our case, which is facilitated by total internal reflection. The modes are solutions of the three-dimensional Maxwell equations. If, however, we assume that the radiation is effectively confined vertically within the active region of our mesa, then we may approximate this situation using a two-dimensional solution which yields Bessel function solutions for the radial field distribution. The effective cavity length of $2\pi R$ imposed by the periodic boundary condition on the circulating wave results in the WG eigenmode condition: $2\pi Rn = m\lambda$ for large integer m, where R is the mesa radius, n is the refractive index, and the mode spacing is simply given by $\Delta\lambda_{WG} = \lambda^2/2\pi Rn$. This enables us to estimate a WG mode spacing of 2.1 nm, which agrees reasonably with the value of 1.7 nm measured experimentally from the spectra of Fig. 1.